Gao, Y., Jia, J., Lu, Y., Zhou, F., Hao, Z., Johnes, P. J., Dungait, J. A. J., & Shi, K. (2020). Cascading multiscale watershed effects on differential carbon isotopic characteristics and associated hydrological processes. *Journal of Hydrology*, *588*, [125139]. https://doi.org/10.1016/j.jhydrol.2020.125139

Cascading multiscale watershed effects on differential carbon isotopic characteristics and associated hydrological processes

Yang Gao[1,3*], Junjie Jia[1,3], Yao Lu[1,3], Feng Zhou[4], Zhuo Hao[1,3], Penny J. Johnes[5], Jennifer A. J. Dungait [6], Kun Shi[2]

1.Key Laboratory of Ecosystem Network Observation and Modeling, Institute of Geographic Sciences and Natural Resources Research, CAS, Beijing 100101, P. R. of China; 2. State Key Laboratory of Lake Science and Environment, Nanjing Institute of Geography and Limnology, CAS, Nanjing 210008, P. R. of China; 3. University of Chinese Academy of Sciences, Beijing, 100049, P. R. of China; 4. Sino-French Institute for Earth System Science, College of Urban and Environmental Sciences, Peking University, Beijing, P. R. of China; 5. School of Geographical Sciences, University of Bristol, University Road, Bristol BS8 1SS, UK; 6. Geography, CLES, Amory Building, University of Exeter, Rennes Drive, Exeter EX4 4RJ UK

Abstract: Understanding land-use change accompanied by anthropogenic activities under alterations in watershed size regulations or differential carbon (C) isotope characteristics remain a challenge in C cycling research. In this study, we investigate changes in the export of C composition and its isotopic characteristics at multiple scales in a subtropical cascading watershed in China. Results show that C concentrations in rainfall and dissolved total carbon (DTC), dissolved organic carbon

E-mail: gaoyang@igsnrr.ac.cn Tel: +86-10-64889040

(DOC) and $\delta^{13}C$ in runoff seasonally fluctuate at a temporal scale. On average, the $\delta^{13}C$ from silicate rock weathering was 31–32%, contributing the largest amount of $\delta^{13}C$ in the different watersheds. Moreover, the contribution of isotopic composition from atmospheric deposition to the $\delta^{13}C$ fraction increased as watershed size increased, while the corresponding contribution from soil organic matter (SOM) decomposition decreased. On the other hand, anthropogenic activities play a dominant role in the isotopic composition of large watersheds. In addition, the correlation coefficient between C transport via runoff and the $\delta^{18}O$ value in rainfall increased as watershed size increased. This indicated that as a source rainfall had an obvious influence on C transport in runoff according to proportional values measured in event and pre-event water.

Keywords: C transport; ^{13}C; watershed; scale effect; hydrological process

1. Introduction

Land-use change causes soil disturbances, which specifically impacts terrestrial ecosystem carbon (C) cycling and C turnover rates (Friend et al., 2014; Ahlström et al., 2015; Atwood et al., 2017). This multiscale disturbance effect on C decomposition and transport remains highly uncertain. In global C cycling, rivers play an important role in transporting C from terrestrial to coastal ecosystems (Gao et al., 2016). This is because biogeochemical cycling, chemical weathering and substance transport are ultimately regulated by the specific runoff processes of different landscapes under the influence of precipitation before reaching stream systems (Segura et al., 2012;

Jasechko et al., 2016). However, the effect that anthropogenic activities have on watershed characteristics that sequentially impact C cycling is still not fully understood due to the complex multiscale nature of C dynamics resulting from hydrological processes.

Watershed runoff is composed of both event water and pre-event water. Thus, runoff-derived C isotope export is dominated by two hydrological processes: water that is stored in a watershed prior to the occurrence of runoff that mainly derives from pre-precipitation events, which is referred to as pre-event water or old water, and water that is input into a watershed from a given precipitation event, which is referred to as event water or young water (Buttle, 1994; Laudon et al., 2007; Klaus and McDonnell, 2013). Influencing factors on isotopic composition in stream water that derive from various hydrological pathways under different watershed sizes are determined by topography, land-use type or landscape pattern (Shanley et al., 2002; Didszun and Uhlenbrook, 2008; James and Roulet, 2009). Therefore, ways in which watershed characteristics impact isotopic composition in runoff can be evaluated by understanding the proportional changes in pre-event and event water that reaches stream systems (Sun et al., 2019).

The sensitivity of annual runoff to forest cover change is significant at multiple spatial scales and tends to decrease as watershed size increases (Zhang et al., 2017; Miao et al., 2016 and 2019). The impact on watershed runoff at multiple spatial scales differs; moreover, the watershed scale in itself can produce the opposite effect on proportional event and pre-event runoff (Zhang et al., 2017; Su et al., 2019). For example, at a large scale, hydrologic watershed processes are dominated by climate change and anthropogenic activities, such as afforestation, deforestation, land-use type and urbanization (Frank et al., 2015; Gao et al., 2020). Klaus and McDonnell (2013) reported that the contribution of pre-event water in small watersheds (i.e., <0.05 km^2) increased as watershed size increased; however, Shanley et al. (2002) hypothesized that pre-event water would in fact decrease with an increase in watershed size. Some studies, such as McGlynn et al. (2004), Laudon et al. (2007) and James and Roulet (2009), also reported that no watershed size effect would occur under a watershed scale range from 0.03 km^2 to 10^4 km^2.

Sun et al. (2019) confirmed the existence of land-use type and spatial pattern scale effects on the isotopic composition of stream water; however, the impact of watershed characteristics on isotopes in stormflow over multiple spatial scales is still unclear. For example, Drake et al. (2019) found that dissolved organic carbon (DOC) transported by river systems under 100% watershed forest cover was in fact event water, whereas DOC transported under watershed deforestation was pre-event water. Sources of dissolved inorganic carbon (DIC) in stream water are mainly determined by the carbon dioxide (CO_2) in soil (through groundwater), chemical weathering, carbonate (rock) dissolution, atmospheric CO_2 exchange and deposition and planktonic respiration (Hao et al., 2019). Therefore, compared to organic and particulate fractions, DIC concentrations and δ^{13}C–DIC values can provide a better understanding of the C sources and processes involved in watershed C cycling (Brunet et al., 2009; Li et al., 2010; Hao et al., 2019).

In this study, we hypothesized that land-use types and landscape patterns linked to changes in watershed size at multiple scales could potentially have a greater effect in regulating differential C isotopic characteristics during runoff processes. The primary aim of this study was to investigate changes in the export of C composition and its isotopic characteristics at multiple scales in a subtropical cascading watershed in China. We focused on two specific objectives: 1) determining how multiscale watersheds regulate C composition and its isotopic characteristics; 2) identifying dominant C sources and associated changes in export processes with respect to watershed size in a cascading watershed.

2. Materials and Methods

2.1 Study area

The cascading watershed selected for this study is in Jiangxi Province, China, located in the middle and lower reaches of the Yangtze River (115°4′13″ E~116°24′6″ E, 26°44′48″ N~29°44′40″ N) (Fig. 1a). Three different watershed scales were selected as study sites, namely, the Poyang Lake watershed (1.67×10^5 km^2), the Ganjiang (Gan) River watershed (8.3×10^4 km^2) and the Jiazhu River watershed (121 km^2) (Fig. 1b). Water from Poyang Lake flows into the middle and lower reaches of the Yangtze River from south to north near Hukou County, Jiujiang City, China. The Ganjiang River is the largest tributary of Poyang Lake, and its runoff volume accounts for 46.6% of the total runoff in the Poyang Lake watershed (Li et al., 2018; Wang et al., 2015). The Jiazhu River is the secondary tributary of the Ganjiang River watershed, which is connected to the Qianyanzhou Ecology Station under the authority of the Chinese Academy of Sciences (CAS).

Poyang Lake influenced by a warm and humid subtropical climate, with an annual mean precipitation of approximately 1622 mm, a mean annual air temperature of 16~20 °C and an annual average relative humidity of 84% (Hao et al., 2018; Gao et al., 2019a). Poyang Lake is typical lake of a water conveyance-type that continuously receive and discharge water, which fed through water conveyance from Yangtze River. Therefore, the complex hydrological processes of the Poyang Lake make it difficult to clearly understand the specific biogeochemical process. The Poyang Lake connected to five major rivers, receiving its water supply from them, wherein the Ganjiang River being the largest tributary of Poyang Lake, contribute 58.4% of runoff to the Poyang Lake.

The Poyang Lake watershed is emblematic of the subtropical, hilly red soil terrain typical of much of Jiangxi Province, China, which is characterized by low hills, hill terraces and valley floodplains. Red soil is the typical soil type found in the study area, which is classified as a mix of oxisols, clay, fine loam, hyperthermic and acidic Udic Cambisols as classified under the United States Department of Agriculture (USDA) soil taxonomy standard (Gao et al., 2014). This study subdivided the Poyang Lake watershed into four land-use types according to the different anthropogenic activities in its surrounding area: cropland, grassland, woodland and water area (Fig. 1b).

2.2 Sample and laboratory analysis

According to the different geomorphic units and spatial distributions, a total of 15, 12 and 3 long-term monitoring points were distributed throughout Poyang Lake, the Ganjiang River and the Jiazhu River, respectively (Jia et al., 2019) (Fig. 1b). Sampling took place from June 2017 to July 2019 at an interim of approximately three months wherein we collected 200 ml of baseflow at a 0~30- cm depth of mixed water samples for laboratory analysis. There were 56 rainfall events collected for C, O, H analysis and 240 runoff sample from Jiazhu River to the Poyang Lake in this study. Water samples were used to determine dissolved inorganic carbon (DIC), dissolved organic carbon (DOC) and dissolved total carbon (DTC) using the TOC Analyzer Ⅱ (vario EL Ⅲ, Germany), and $\delta^{13}C_{DIC}$ was determined using the Finnigan MAT-252 mass spectrometer (Thermo Fisher Scientific, Darmstadt, Hesse, Germany). Stable isotopic composition is an ideal index capable of two-component (δD and $\delta^{18}O$) separation (Penna et al., 2014).

2.3 Data analysis

2.3.1 ^{13}C, δD and ^{18}O isotope calculation

The C, D and O isotopic ratios expressed as delta values are as follows:

$$\delta^{y}X\ (‰) = \left(\frac{R_{sample}}{R_{ref.std.}} - 1\right) \times 1000 \qquad (1)$$

where X represents the target isotope; y represents the number of atoms; R_{sample} and $R_{standard}$ represent the ratio of heavy to light isotopes in the samples and the standard references. For isotopic O measurements, we used the Vienna Standard Mean Ocean Water (VSMOW) standard, distributed by the International Atomic Energy Agency (IAEA) in Vienna, Austria, for which uncertainty was no greater than ±0.1‰

and was only ±2‰ for δD measurements; C isotope data were reported on the Vienna Pee Dee Belemnite (VPDB) (‰) scale, with a standard deviation (1σ) of 0.15‰ (Zhao et al., 2019).

2.3.2 Isotopic mixing model

Under one isotope system and three sources, we used the following system for mass balance equations to determine the proportions (f_A, f_B and f_c) of isotopic source signatures (δ_A, δ_B and δ_c), coinciding with the observed signature of the mixture (δ_M):

$$\delta_M = f_A\delta_A + f_B\delta_B + f_C\delta_C \cdots$$

$$1 = f_A + f_B + f_C \cdots$$

However, under n (A, B, C…) isotope systems and > n+1 sources, we were still able to use the requirement for mass balance conservation to determine multiple combinations of source proportions, which is a feasible solution. IsoSource, a multi-source mixing model (freely available at http://www.epa.gov/wed/pages/models.htm), was used to calculate the contribution of each water source under consideration to the recorded C pools (Phillips and Gregg, 2003; Phillips et al., 2005).

3. Results

3.1 C dynamic change in rainfall

As shown in Fig. 2a, C concentrations in rainfall fluctuated, wherein high DTC, DIC and DOC concentrations in rainwater were observed during the dry season (from winter to spring), yielding two peak values during this period that reached 10~30 mg/L. Greater than 70% of DTC in rainwater ranged from 2.5 to 9 mg/L, whereas 80% of the DIC concentration in rainwater was below 5 mg/L and most of the DOC concentration in rainwater was evenly distributed (from 0.29 to 10 mg/L) (Fig. 2b). From June 2017 to July 2019, the DTC concentration in rainwater was 7.13±5.25 mg/L, the DIC concentration in rainwater was 3.04±2.49 mg/L and the DOC concentration in rainwater was 4.09±3.15 mg/L. From June 2017 to July 2019, most rainfall in the study area was concentrated in spring and summer, namely, 442.9± 164.7 mm and 619.5±62.1 mm, respectively (Fig. 2c).

3.2 C Spatiotemporal change in runoff

As shown in Fig. 3a, In the Jiazhu River, fluctuations in DTC concentrations ranged from 4.9 to 7.1 mg/L from upstream to downstream, whereas the Ganjiang River exhibited irregular fluctuations under seasonal change. Specifically, fluctuations in DTC concentrations in the downstream area of this river (i.e., into Poyang Lake) increased to 7.4 mg/L. For Poyang Lake, fluctuations in DTC concentrations also exhibited regional change, wherein the northern section on the lake (from P9 to P14, i.e., into Yangtze River) only ranged from 1.9 to 4.2 mg/L, which was significantly less than that measured at other sample points. On a spatial scale, DTC concentrations gradually increased from the Jiazhu River (13.7±6.1 mg/L) to Poyang Lake (14.4±5.0 mg/L) (Fig. 3a).

Seasonal changes in DIC concentrations showed an irregular trend, which differed from changes in DTC concentrations. Moreover, DTC concentrations during the rainy season (from July to September) also yielded high values (Fig. 3b). From the

Jiazhu River to Poyang Lake, fluctuations in DTC concentrations mainly ranged from 1.3 to 4.7 mg/L, with an average of 2.4±0.8 mg/L. Moreover, DTC concentrations (with an average of 8.7±2.2 mg/L) were higher in the Ganjiang River compared to the Jiazhu River and Poyang Lake, with an average of 7.7±2.6 mg/L and 8.0±2.5 mg/L, respectively.

Specifically, fluctuations in DOC concentrations in the Jiazhu River were higher than the Ganjiang River and Poyang Lake, with an average of 4.7±1.1 mg/L (Fig. 3c). Moreover, DOC concentrations exhibited differing spatial distribution characteristics, wherein DOC concentrations in Poyang Lake were far higher than those in either the Jiazhu and Ganjiang rivers, reaching 6.4±3.1 mg/L. The DOC concentration of the Ganjiang River (5.5±3.4 mg/L) was less than that of the Jiazhu River (6.0±4.7 mg/L), particularly from the midstream sampling points of the Ganjiang River (from G3 to G10; only 4.2 to 5.7 mg/L, respectively).

3.3 Seasonal changes in $\delta^{13}C$ values from rainfall to runoff

As shown in Fig. 4a, the $\delta^{13}C$ values in runoff from June 2017 to July 2019 showed seasonal differences, and on the whole, the $\delta^{13}C$ values exhibited significant seasonal fluctuation, reaching -13.0±5.1‰. wherein the $\delta^{13}C$ values on May 19 and September 18 were -8.8±1.0‰ and -11.6±0.9‰, respectively; however, the $\delta^{13}C$ values on January 19 and July 19 were -13.9±1.4‰ and -15.4±1.7‰, respectively. From the Jiazhu River to Poyang Lake, the $\delta^{13}C$ values exhibited a gradual decreasing trend. The $\delta^{13}C$ value in the Jiazhu River was -13.5±3.2‰, but the $\delta^{13}C$ value in the Ganjiang River was only -12.2±3.1‰. Moreover, $\delta^{13}C$ values in water flow entering into Poyang Lake reached -12.6±3.1‰. The $\delta^{13}C$ values in rainfall also exhibited seasonal variation, ranging from -5.1‰ on April 18 to -10‰ on August 18; however, the $\delta^{13}C$ values in rainfall ranged from -11.8‰ on September 19 to -27.1‰ on March 19 (Fig. 4b).

4. Discussion

4.1 C source analysis on a spatiotemporal scale

According to the $\delta^{13}C$ values measured from rainfall to runoff, we further analyzed differences in C sources from the Jiazhu River to Poyang Lake using an isotopic mixing model (Fig. 5). Many environmental and internal factors can impact $\delta^{13}C$ values in watersheds, such as carbonate mineral dissolution, atmospheric precipitation, soil organic matter (SOM) and groundwater inputs (Shin et al., 2011; Hao et al., 2019). In this study, we focused on the four main sources, including silicate rock weathering, carbonate rock weathering, SOM decomposition and atmospheric deposition. This can be explained by the fact that silicate rock and carbonate rock are two main minerals that comprise red soil (Gao et al., 2014).

As Fig.5a shown, the $\delta^{13}C$ that derived from silicate rock weathering, with an average contribution of 31–32%, is the largest source for DTC in these three cascading watersheds; however, the $\delta^{13}C$ that derived from atmospheric deposition as well as from a certain amount of SOM decomposition are the second largest sources of these three cascading watersheds, with an average contribution of 24–29%. The contribution of atmospheric deposition to the $\delta^{13}C$ fraction increased with an increase in watershed size, while the contribution of SOM decomposition decreased. The contribution of carbonate rock weathering to the $\delta^{13}C$ fraction exhibited the largest fluctuation from summer to autumn (Fig. 5b). This is because the percentage of subsurface runoff will supplement and subsequently increase carbonate reactions to occur in streamflow in autumn when streamflow typically decreases (Yan et al., 2014; Zhao et al., 2010). Therefore, pre-event (old) water in matrix pores comes into play, which is more enriched in $\delta^{13}C$ due to the longer time required for calcium carbonate ($CaCO_3$) dissolution.

In addition, from winter to spring, atmospheric deposition is the main source of $\delta^{13}C$, contributing 33–35%; however, during the rainy season, rock weathering and SOM decomposition are the main $\delta^{13}C$ sources under heightened rainfall conditions (Fig. 5b). The isotopic results from this study correspond well with recent research on controlling mechanisms associated with SOM decomposition, wherein environmental changes and landscape disturbances have resulted in the export of aged, aliphatic, protein-like and microbial dissolved organic matter (DOM) content (Wilson and Xenopoulos, 2008; Wagner et al., 2015; Creed et al., 2018). As report by Wang et al (2014), the $\delta^{13}C$-DIC C values in the sediment in Poyang Lake area were -22.48 ± 4.10‰, being close to the average SOM value with 24‰ in China, so in present study, the lake sediment and SOM under different watershed size derived from the same source.

The interactions between land use change at different scale and runoff have always been studied nearly a century. In this study, the runoff is also main driving factor for C and its isotopic transformation in cascading multiscale watershed. We also get a general conclusion from this research that at small size of watershed like Jiazhuhe River and Ganjiang watershed, human activities, such as deforestation, harvesting, urbanization and land cover change, would increase annual mean runoff but afforestation decrease streamflow in the opposite way, with Zhang et al (2015), Carvalho-Santos et al (2016) and Buendia et al (2016). However, at large scale like whole the Poyang Lake, the hydrological regime and precipitation would be more sensitive factors on runoff (Zhang et al., 2017), but the increase of the vegetation impact on C by runoff at both large and small scale of watershed. Therefore, we think as change of watershed size, land use and related vegetation pattern play a predominant role in regulating the isotopic C compositions in runoff in watersheds within areas ranging from 100 km^2 to 10000 km^2.

4.2 Hydrological processes associated with C transport

In this study, we compared the Global Meteoric Water Line (GMWL) and the Local Meteoric Water Line (LMWL) for the entire Poyang Lake watershed (i.e., all three cascading watersheds) based on measured D and O isotopes in precipitation from June 2017 to July 2019 using the least squares method. The GMWL ($\delta D = 8\delta^{18}O+10$) was taken from Hao et al. (2018), which is the black line shown in Fig. 6a. The intercept of the correlation line can reflect the unbalanced status of evaporation in water vapor formation (Hao et al., 2018). The slope and the interception of the LMWL were close to the GMWL, which confirmed the same humid and moist origin (Fig. 6a).

In comparison to the LMWL, the lower slope and the intercept of the Local

Runoff Water Line (LRWL) implied the absorption of evaporated water, which can be explained by that found in the low latitude area; thus, the watershed undergoes higher and more intensive evaporation due to the overall high temperature and the strong solar radiation. The LRWL slopes of the Jiazhu River, the Ganjiang River and Poyang Lake watersheds were similar, suggesting that the relative air humidity was the same for all three watersheds, but the interception for Poyang Lake was different from the other two. This is because the Jiazhu River and the Ganjiang River watersheds are representative of an unbalanced status in water vapor evaporation formation, while the Poyang Lake is representative of a relatively balanced status under increased water area and runoff input sources. Moreover, this also reflects the differences in precipitation sources for the LRWL between the rivers and the lake.

The range of slopes was extensive in stream water isotopic composition for all three watersheds, which was determined using the composition of event and pre-event water samples and their respective proportions (Tetzlaff et al., 2011; Klaus and McDonnell, 2013). As watershed size changes, the isotopic composition of small scale watersheds will be more easily influenced by complex runoff processes, such as translatory flow, piston-like flow, preferential flow and subsurface storage (Sun et al., 2019); whereas in large watersheds, like Poyang Lake, anthropogenic activities, such as aquaculture, fishing, algaculture and land reclamation, will dominate the isotopic composition.

4.3 Coupled C–H_2O watershed processes

The varying isotopic composition of the watersheds could be attributable to the diversity in the extent of assimilation of event water isotopes and/or the delivery of stored water isotopes in different runoff pathways for the different sized watersheds (Sun et al., 2019). Moreover, rainfall events can activate and connect hydraulically disconnected preferential pathways (Spence et al., 2010; Sayama et al., 2011). In this study, C transport under different land-use types and associated land-use patterns was partly driven by rainfall events across multiple scales. As shown in Fig.7a, the correlation coefficient between DTC in runoff and the $\delta^{18}O$ value in rainfall, ranging from 18% to 28%, was approaching that of the atmospheric deposition contribution for $\delta^{13}C$ in the watersheds, ranging from 26% to 28% as shown in Fig. 6a. In addition, the correlation coefficient increased with increasing watershed size. These results also indicated that rainfall had an obvious influence on the DTC transport source via runoff generation according to proportional values measured in event and pre-event water. The correlation between DIC changes in the watersheds and the $\delta^{18}O$ value in rainfall was unbalanced, and watershed size effects were not observed (Fig.7b). This can be explained by the fact that DIC changes are dominated by silicate rock and carbonate rock weathering, making precipitation an important driving factor.

There was a significant correlation between changes in DOC in runoff with an increase in watershed size (R^2=0.48) to changes in $\delta^{18}O$ in rainfall (Fig.7c). This is because the rainfall event water fraction could potentially increase during SOM decomposition that would in turn drive DOC transport via rainfall. In addition, an increase in anthropogenic activities with an increase in watershed size will alter aboveground and belowground DOC pathways (Oshun et al., 2016; Yang et al., 2018).

Moreover, the DOC characteristics mobilized in large watersheds are also higher than DOC exported from small watersheds, indicating potential vulnerability in microbial degradation (Drake et al., 2019). The chemodiversity of DOC, defined as the presence and proportion of C, O and hydrogen (H), is an important indicator of both DOC sources and DOC quality (Wagner et al., 2015). Our research has shown that anthropogenic activities impact DOC export in these watersheds by inducing a greater relative abundance in isotopic O and H composition (D'Andrilli et al., 2015; Riedel et al., 2016).

The lower correlation found between $\delta^{13}C$ and $\delta^{18}O$ compared to that of DOC and $\delta^{18}O$ is assumed to be attributable to rock weathering being the main source of $\delta^{13}C$ in runoff, while rainfall is assumed to enhance the proportion of event and pre-event water (Fig. 7d). In addition, the correlation between $\delta^{13}C$ and $\delta^{18}O$ was shown to decrease with an increase in watershed size, which could be partly explained by the fact that more complex land-use types and anthropogenic activities cause variation in the proportion of event and pre-event water in runoff and isotopic composition.

4.4 Isotopic C characteristics in C runoff export

Further analysis of the correlation between C and its associated isotopes only showed an approaching correlation coefficient between different forms of C and $\delta^{13}C$ in runoff with an R^2 range of 0.15~0.18 (Fig. 8). This is because the $\delta^{13}C$ values in runoff were mostly higher than the average photosynthetic pathway value of C3 plants, ranging from -21‰ to -35‰, and approaching that of C4 plants, ranging from -10‰ to -14‰ (Rouw et al., 2015). These results also implied that sable water cycles and isotopic flow mainly impact differential characteristics of C export via the watershed size effect. It has been suggested that the lower contribution of vegetation to $\delta^{13}C$ in runoff and ^{13}C tends to concentrate in root systems followed by twigs and leaves, but lighter ^{12}C isotopes are released from plants through transpiration (Hao et al., 2019). Future research should therefore focus more on hydrological or hydrochemical C processes at multiple scales as well as associated water sources, pathways and residence times and the impact of land-use types and patterns and anthropogenic activities on isotopic C cycle processes.

As shown in Fig.9, the surface water with the pH values ranged from 6.0 to 8.2. The pH for the Jiazhu River and the Ganjiang River were slightly higher than that of Poyang Lake. In general, the correlations between dissolved carbon and pH, $\delta^{13}C$ and pH in surface water were low, and the correlation coefficients decreased with increasing watershed size (Fig. 9), which could be partly explained by the fact that more complex land-use types and anthropogenic activities diluted the effect of pH on dissolved carbon. In addition, we observed a significant negative correlation between DOC and pH value in the runoff of the Jiazhu river (R^2=0.36, $P<0.05$), but no such trend in the larger watersheds, which might be related to the input of hydrophilic acid organic matter in the farmland of the Jiazhu River Basin.

5. Conclusions

This study set out to confirm whether the watershed size effect has an influence on C and differential C isotopic characteristics via runoff. Results showed that the contribution of atmospheric deposition to the $\delta^{13}C$ fraction increased with an increase in watershed size, while the contribution of SOM decomposition decreased. As the size of the watershed increases, land-use patterns and related vegetation pattern under anthropogenic activities play a predominant role in regulating the isotopic C compositions in runoff in watersheds . The correlation coefficient between C transport via runoff and the $\delta^{18}O$ value in rainfall increased with increasing watershed size, particularly for DOC, which was significantly correlated. Owing to the fact that watershed ecosystems will be the main field of C cycling research in future studies, more focus must be paid to effects associated with land-use patterns and anthropogenic activities on C flow and isotopic composition regulation at multiple watershed scales.

Acknowledgments

The authors of this study would like to thank all anonymous reviewers for their helpful remarks. This study was financially supported by the National Nature Science Foundation of China (No. 41922003, 41871080 and 41830860).

References:

Ahlström, A., Xia, J., Arneth, A., Luo, Y., Smith, B., 2015. Importance of vegetation dynamics for future terrestrial carbon cycling. Environ. Res. Lett. 10, 054019.

Atwood, T.B., Connolly, R.M., Almahasheer, H., Carnell, P.E., Duarte, C.M., Lewis, C.J.E., Irigoien, X., Kelleway, J.J., Lavery, P.S., Macreadie, P.I., Serrano, O., Sanders, C.J., Santos, I., Steven, A.D.L., Lovelock, C.E., 2017. Global patterns in mangrove soil carbon stocks and losses. Nat. Clim. Change 7, 523–528.

Brunet, F., Dubois, K., Veizer, J., Ndondo, G.R.N., Ngoupayou, J.R.N., Boeglin, J.L., Probst, J.L., 2009. Terrestrial and fluvial carbon fluxes in a tropical watershed: Nyong basin, cameroon. Chem. Geol. 265 (3), 563–572.

Buendia, C., Batalla, R.J., Sabater, S., Palau, A., Marcé, R., 2016. Runoff trends driven by climate and afforestation in a pyrenean basin. Land Degrad. Dev. 27 (3), 823–838.

Buttle, J., 1994. Isotope hydrograph separations and rapid delivery of pre-event water from drainage basins. Prog. Phys. Geog. 18(1), 16-41.

Carvalho-Santos, C., Nunes, J.P., Monteiro, A.T., Hein, L., Honrado, J.P., 2016. Assessing the effects of land cover and future climate conditions on the provision of hydrological services in a medium-sized watershed of Portugal. Hydrol. Process. 30 (5), 720-738.

Creed, I.F., Bergström, A., Trick, C.G., Grimm, N.B., Hessen, D.O., Karlsson, J., Kidd, K.A., Kritzberg, E., McKnight, D.M., Freeman, E.C., Senar, O.E., Andersson, A., Ask, J., Berggren, M., Cherif, M., Giesler, R., Hotchkiss, E.R., Kortelainen, P., Palta, M.M., Vrede, T., Weyhenmeyer, G.A., 2018. Global change-driven effects on dissolved organic matter composition: implications for food webs of northern lakes. Glob. Change Biol. 24, 3692–3714.

D'Andrilli, J., Cooper, W.T., Foreman, C.M., Marshall, A.G., 2015. An ultrahigh-resolution mass spectrometry index to estimate natural organic matter lability. Rapid Commun. Mass Spectrom. 29, 2385–2401.

Didszun, J., Uhlenbrook, S., 2008. Scaling of dominant runoff generation processes:

Nested catchments approach using multiple tracers. Water Resour. Res. 44(2).

Drake, T.W., Oost, K.V., Barthel, M., Bauters, M., Hoyt, A.M., Podgorski, D.C., Six, J., Boeckx, P., Trumbore, S.E., Ntaboba, L.C., Spencer, R.G.M., 2019. Mobilization of aged and biolabile soil carbon by tropical deforestation. Nat. Geosci. 12, 541–546.

Frank, D.C., Poulter, B., Saurer, M., Esper, J., Huntingford, J., 2015. Water-use efficiency and transpiration across European forests during the Anthropocene. Nat. Clim. Change 5, 579–583.

Friend, A.D., Lucht, W., Rademacher, T.T., Keribin, R., Betts, R., Cadule, P., Ciais, P., Clark, D.B., Dankers, R., Falloon, P.D., Ito, A., Kahana, R., Kleidon, A., Lomas, M.R., Nishina, K., Ostberg, S., Pavlick, R., Peylin, P., Schaphoff, S., Vuichard, N., Warszawski, L., Wiltshire, A., Woodward, F.I., 2014. Carbon residence time dominates uncertainty in terrestrial vegetation responses to future climate and atmospheric CO2. Proc. Natl. Acad. Sci. USA 111, 3280–3285.

Gao, Y., He, N.P., Yu, G.R., Chen, W.L., Wang, Q.F., 2014. Long-term effects of different land use types on C, N, and P stoichiometry and storage in subtropical ecosystems: a case study in China. Ecol. Eng. 67, 171-181.

Gao, Y., Yu, G.R., Yang, T.T., Jia, Y.L., He, N.P., Zhuang, J., 2016. New insight into global blue carbon estimation under human activity in land-sea interaction area: a case study of China. Earth-Sci. Rev. 159, 36–46.

Gao, Y., Zhou, F., Ciais, P., Miao, C.Y., Yang, T., Jia, Y.L., Zhou, X.D., Klaus, B.B., Yang, T.T., Yu, G.R., 2020. Human activities aggravate nitrogen deposition pollution to inland water over China. Natl. Sci. Rev. 7, 430–440.

Gao, Y., Hao, Z., Han, N., Yang, J., Zhang, L., Tian, J., Song, X.W., Wen, X.F., He, N.P., 2019a. Tracking the fate of deposited nitrogen and its redistribution in a subtropical watershed in China. Ecohydrology e2094.

Hao, Z., Gao, Y., Sun, X.M., Wen, X.F., 2018. Differential isotopic characteristics of eco-hydrologic processes in a subtropical watershed, China. Ecohydrology 11(1-4), e1944.

Hao, Z., Gao, Y., Ma, M.Z., Green, S.M., Wang, J., Song, X.W., Dungait, J.A.J., Johnes, P., Xiong, B.L., Quine, T.A., Sun, X.M., Wen, X.F., He, N.P., 2019. Using $\delta^{13}C$ to reveal the importance of different water transport pathways in two nested karst basins, Southwest China. J. Hydrol. 571, 425-436.

James, A.L., Roulet, N.T., 2009. Antecedent moisture conditions and catchment morphology as controls on spatial patterns of runoff generation in small forest catchments. J. Hydrol. 377(3), 351-366.

Jasechko, S., Kirchner, J.W., Welker, J.M., McDonnell, J.J., 2016. Substantial proportion of global streamflow less than three months old. Nature Geoscience, 9: 126

Jia, J.J., Gao, Y., Song, X.W., Chen, S.B., 2019. Characteristics of phytoplankton community primary productivity response to the nutrient status of the Poyang Lake-Gan River Basin, China. Ecohydrology 12, e2136.

Klaus, J., McDonnell, J.J., 2013. Hydrograph separation using stable isotopes: Review and evaluation. J. Hydrol. 505(24), 47-64.

Laudon, H., Sjöblom, V., Buffam, I., Seibert, J., Mörth, M., 2007. The role of catchment scale and landscape characteristics for runoff generation of boreal streams. J. Hydrol. 344(3), 198-209.

Li, S.L., Liu, C.Q., Li, J., Lang, Y.C., Ding, H., Li, L.B., 2010. Geochemistry of dissolved inorganic carbon and carbonate weathering in a small typical karstic catchment of Southwest China: isotopic and chemical constraints. Chem. Geol. 277, 3–4.

Li, C.Q., Wang, P., Chen, B., Li, Y., 2018. Spatial distribution and pollution source of dissolved metals in the Ganjiang River of Lake Poyang Basin. Journal of Lake Sciences 30, 139-149. (In Chinese)

Miao C.Y., Kong D.X., Wu J.W., Duan Q.Y., 2016. Functional degradation of the water–sediment regulation scheme in the lower Yellow River: Spatial and temporal analyses. Science of the Total Environment, 551-552: 16-22.

Miao C.Y., Duan Q.Y., Sun Q.H., Lei X.H., Li H., 2019. Non-uniform changes in different categories of precipitation intensity across China and the associated large-scale circulations. Environmental Research Letters, 14, DOI: 10.1088/1748-9326/aaf306.

McGlynn, B.L., McDonnell, J.J., Seibert, J., Kendall, C., 2004. Scale effects on headwater catchment runoff timing, flow sources, and groundwater-streamflow relations. Water Resour. Res. 40(7), W07504.

Oshun, J., Dietrich, W.E., Dawson, T.E., Fung, I., 2016. Dynamic, structured heterogeneity of water isotopes inside hillslopes. Water Resour. Res. 52, 164-189.

Penna, D., Engel, M., Mao, L., Dell'Agnese, A., Bertoldi, G., Comiti, F., 2014. Tracer-based analysis of spatial and temporal variations of water sources in a glacierized catchment. Hydrol. Earth Syst. Sc. 18(12), 5271-5288.

Phillips, D.L., 2003. Source Partitioning Using Stable Isotopes: Coping with Too Many Sources. Oecologia 136, 261-269.

Phillips, D.L., Newsome, S.D., Gregg, J.W., 2005. Combining sources in stable isotope mixing models: alternative methods. Oecologia 144, 520-527.

Riedel, T. Zark, M., Vähätalo, A., Niggemann, J., Spencer, R., Hernes, P., Dittmar, T., 2016. Molecular signatures of biogeochemical transformations in dissolved organic matter from ten world rivers. Front. Earth Sci. 4, G01004.

Rouw, A., Soulileuth, D., Huon, B.S., 2015. Stable carbon isotope ratios in soil and vegetation shift with cultivation practices (Northern Laos). Agric. Ecosyst. Environ. 200, 161–168.

Sayama, T., McDonnell, J.J., Dhakal, A., Sullivan, K., 2011. How much water can a watershed store? Hydrol. Process. 25(25), 3899-3908.

Segura, C., James, A.L., Lazzati, D., Roulet, N.T., 2012. Scaling relationships for event water contributions and transit times in small-forested catchments in Eastern Quebec. Water Resour. Res., 48(7): W07502

Shanley, J.B., Kendall, C., Smith, T.E., Wolock, D.M., McDonnell, J.J., 2002. Controls on old and new water contributions to stream flow at some nested catchments in Vermont, USA. Hydrol. Process. 16(3), 589-609.

Shin, W.J., Chung, G.S., Lee, D., Lee, K.S., 2011. Dissolved inorganic carbon export from carbonate and silicate catchments estimated from carbonate chemistry and δ^{13}CDIC. Hydrol. Earth Syst. Sci. 15 (8), 2551–2560.

Spence, C., Guan, X.J., Phillips, R., Hedstrom, N., Granger, R., Reid, B., 2010. Storage dynamics and streamflow in a catchment with a variable contributing area. Hydrol. Process. 24(16), 2209-2221.

Sun, L., Yen, H., Chen, L.D., Zhao, F.K., Yang, L., 2019. Distribution of agricultural land regulates water isotopes over multiple stream spatial scale in a subtropical forested watershed. J. Hydrol. doi.org/10.1016/j.jhydrol.2019.124206.

Su, L., Miao C.Y., Duan Q.Y., Lei X.H., Li H., 2019. Multiple-wavelet coherence of world's large rivers with meteorological factors and ocean signals. Journal of Geophysical Research: Atmospheres, DOI: 10.1029/2018JD029842

Tetzlaff, D., Soulsby, C., Hrachowitz, M., Speed, M., 2011. Relative influence of upland and lowland headwaters on the isotope hydrology and transit times of larger catchments. J. Hydrol. 400(3), 438-447.

Wagner, S., Riedel, T., Niggemann, J., Vähätalo, A., Dittmar, T., Jaffe, R., 2015. Linking the molecular signature of heteroatomic dissolved organic matter to watershed characteristics in world rivers. Environ. Sci. Technol. 49, 13798–13806.

Wang, M., Lai, J., Hu, K., Zhang, D., Lai, J., 2014. Compositions and sources of stable organic carbon and nitrogen isotopes in surface sediments of Poyang Lake. China Environmental Science 34, 1019-1025. (in Chinese)

Wang, P., Qi, S.H., Chen, B., 2015. Influence of land use on river water quality in the Ganjiang basin. Acta Ecologica Sinica 35, 4326-4337. (In Chinese)

Wilson, H.F., Xenopoulos, M.A., 2008. Effects of agricultural land use on the composition of fluvial dissolved organic matter. Nat. Geosci. 2, 37–41.

Yan, Y., He, N.P., Yu, G.R., Chen, W.L., Wang, Q.F., 2014. Long-term effects of different land use types on C, N, and P stoichiometry and storage in subtropical ecosystems: a case study in China. Ecol. Eng. 67, 171-181.

Yang, L., Zhang, H.D., Chen, L.D., 2018. Identification on threshold and efficiency of rainfall replenishment to soil water in semi-arid loess hilly areas. Sci. China Earth Sci. 61(3), 292-301.

Zhang, X.K., Fan, J.H., Cheng, G.W., 2015. Modelling the effects of land-use change on runoff and sediment yield in the Weicheng River watershed, Southwest China. J. Mount. Sci. 12 (2), 434–445.

Zhang, M.F., Liu, N., Harper, R., Li, Q., Liu, K., Wei, X.H., Ning, D.Y., Hou, Y.P., Liu, S.R., 2017. A global review on hydrological responses to forest change across multiple spatial scales: Importance of scale, climate, forest type and hydrological regime. J. Hydrol. 546, 44–59.

Zhao, M., Zeng, C., Liu, Z.H., Wang, S.J., 2010. Effect of different land use/land cover on karst hydrogeochemistry: A paired catchment study of Chenqi and Dengzhanhe Puding, Guizhou, SW China. J. Hydrol. 388 (1–2), 121–130.

Zhao, G.Q., Gao, Y., Wang, L., Hao, Z., Wen, X.F., Song, X.W., 2019. Isotopically-tracked hydrological changes in carbon cycling and its sources in a

Chinese subtropical forested watershed. J. Hydrol. 575, 1041–1051.

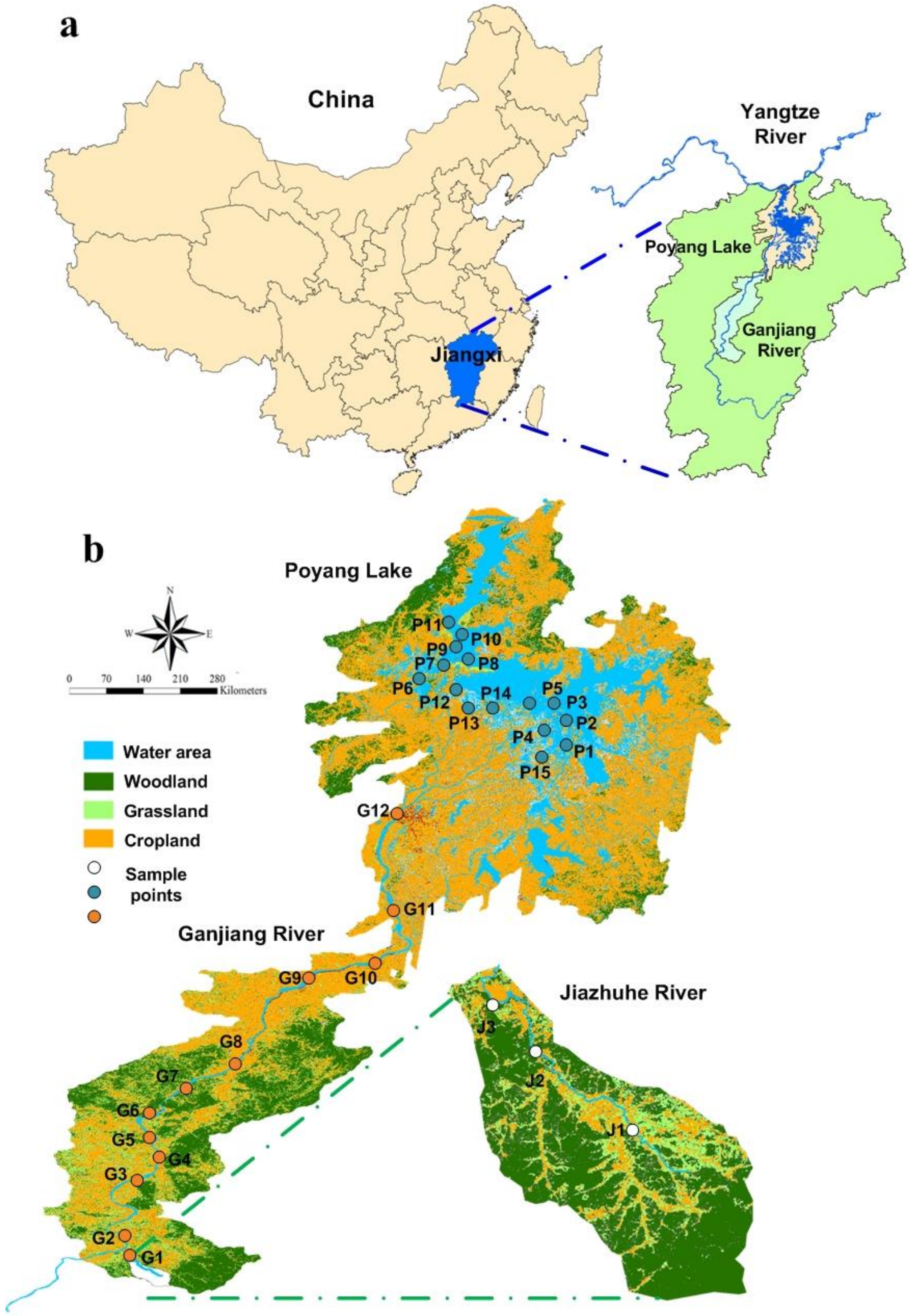

Fig. 1 Location of the Poyang Lake and the Ganjiang River watersheds (a) and sample points and their land-use patterns (b).

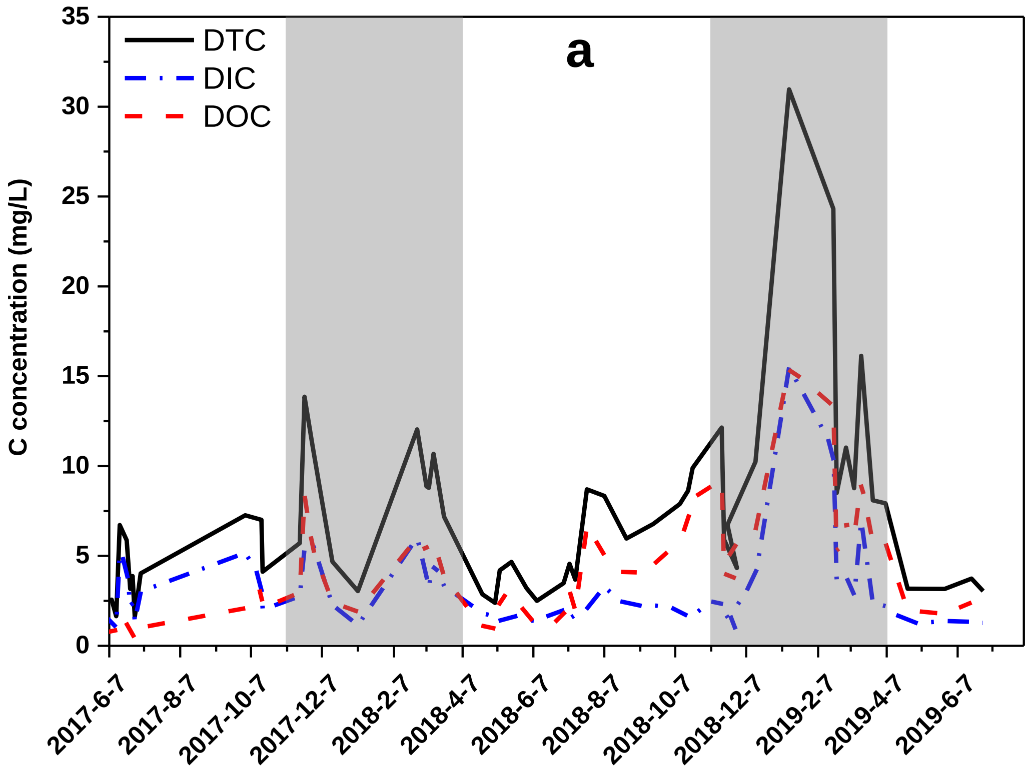

DTC
DIC
DOC
a
C concentration (mg/L)
35
30
25
20
15
10
5
0
2017-6-7
2017-8-7
2017-10-7
2017-12-7
2018-2-7
2018-4-7
2018-6-7
2018-8-7
2018-10-7
2018-12-7
2019-2-7
2019-4-7
2019-6-7

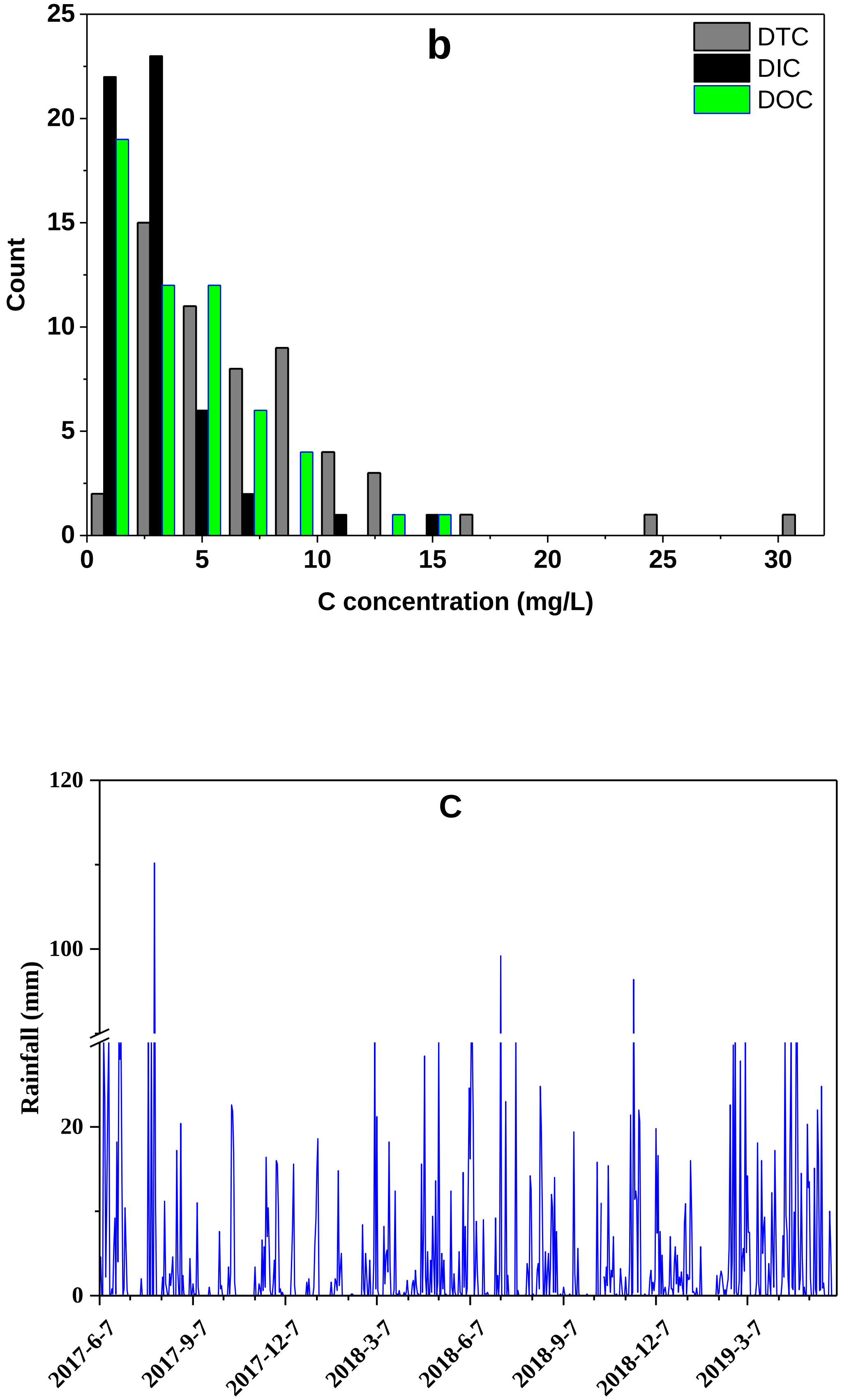

Fig. 2 Changes in carbon concentrations in rainfall (a), and statistics on

changes in C concentrations in rainfall (b) and rainfall fluctuation throughout 2017~2019.

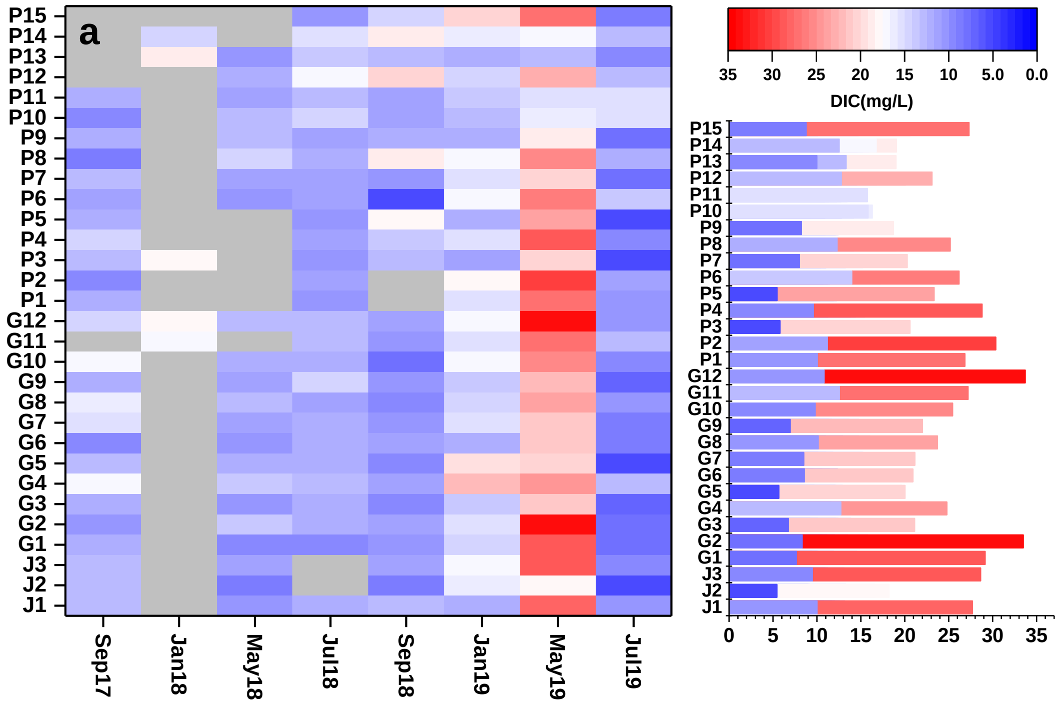

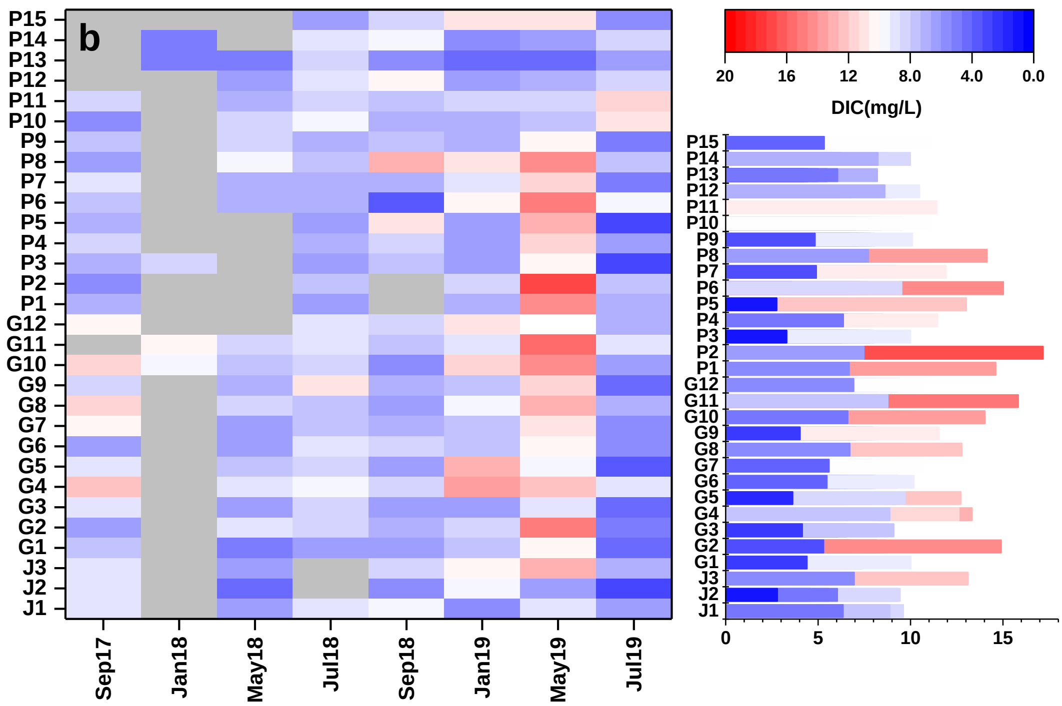

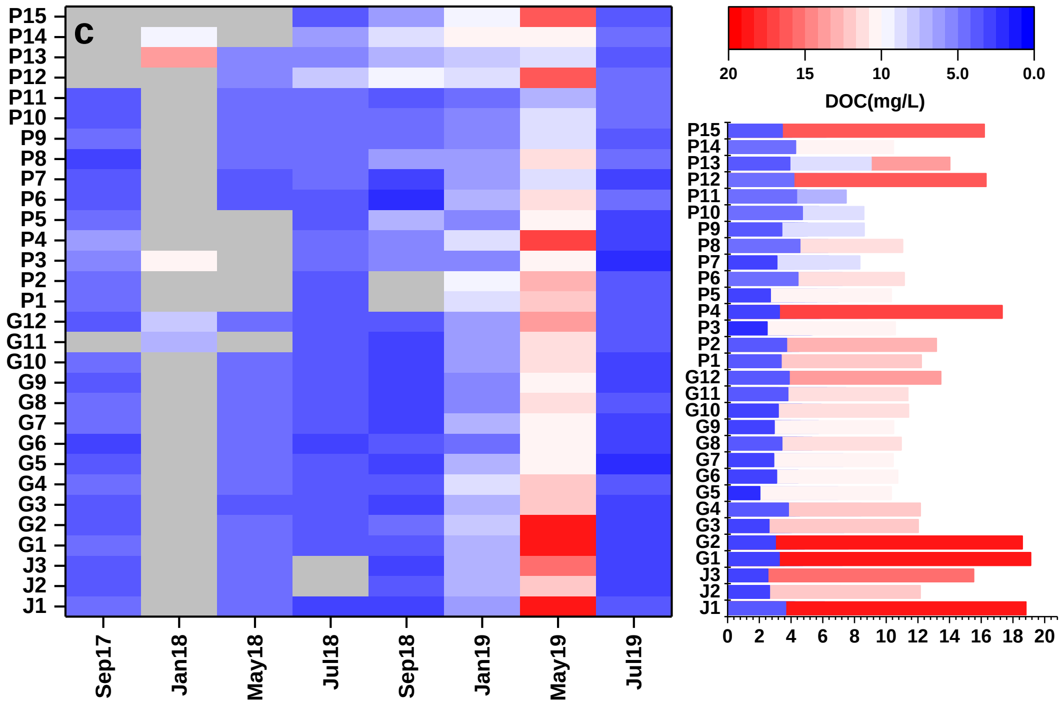

Fig. 3 Dynamic spatiotemporal changes of different carbon forms from the Jiazhu River to Poyang Lake between 2017 and 2019 wherein gray squares represent default values.

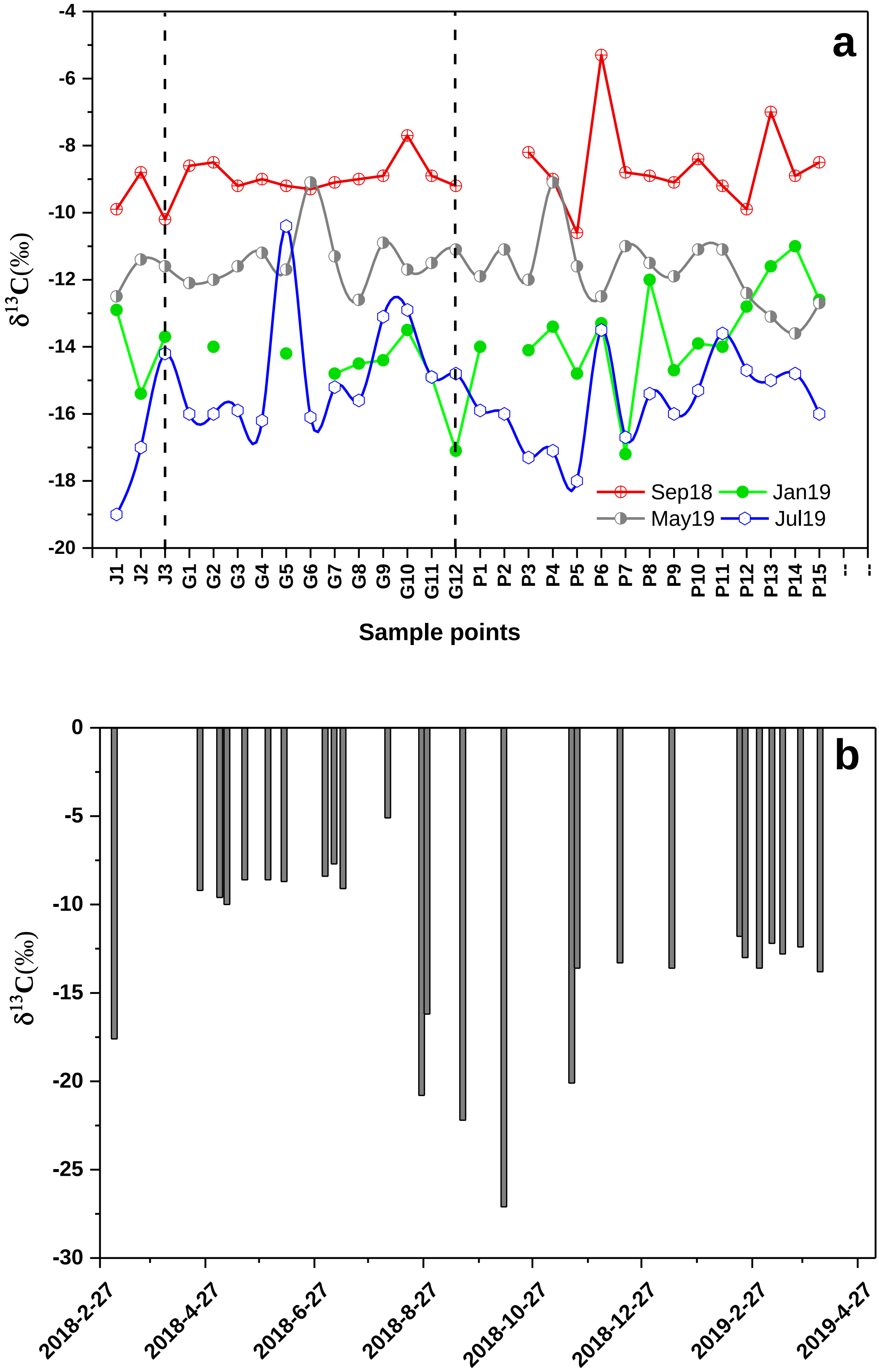

Fig. 4 Seasonal changes in δ^{13}C values from the Jiazhu River to Poyang Lake (a) and in rainfall throughout 2018~2019.

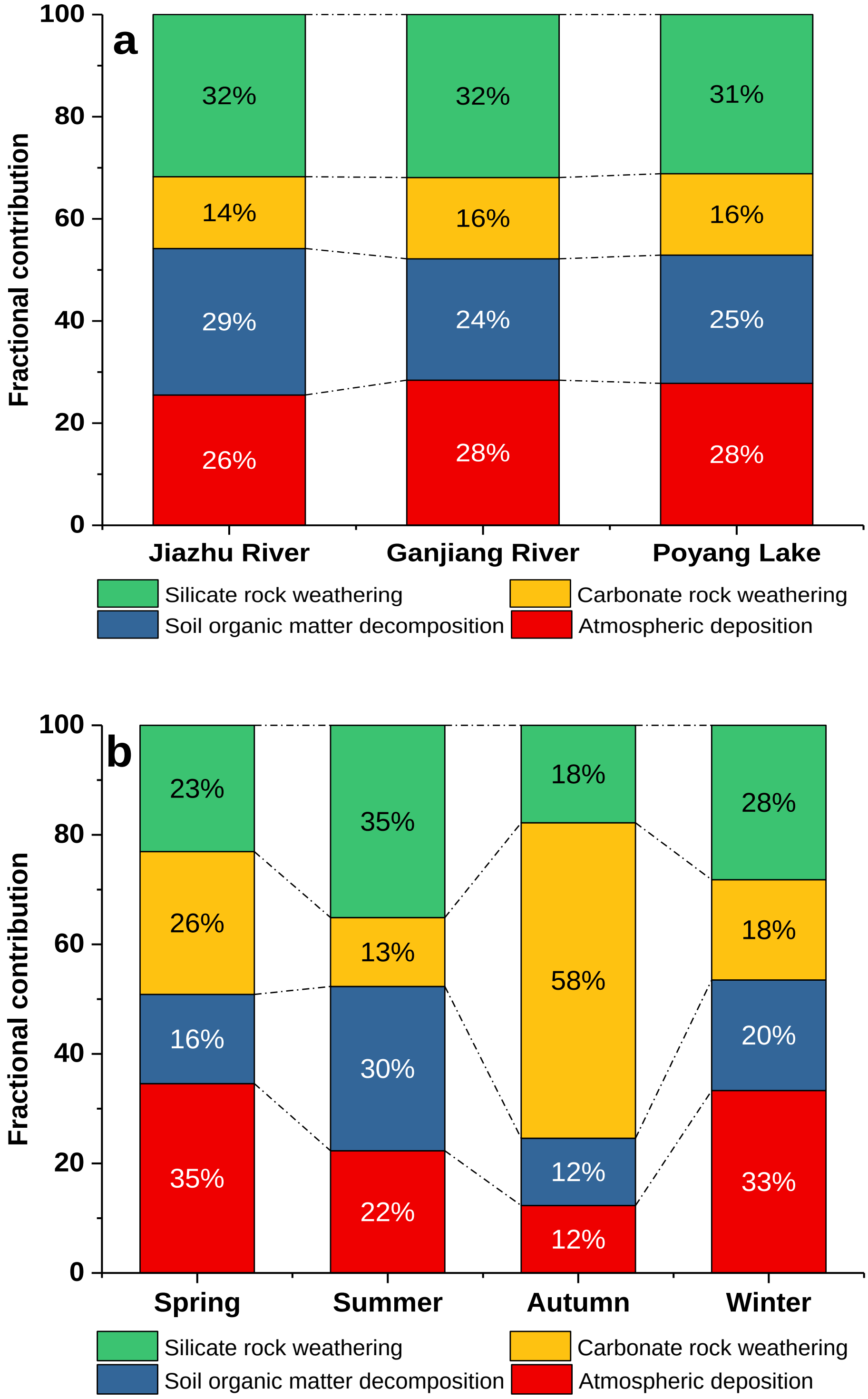

Fig. 5 Carbon source analysis during the rainy and dry seasons for the three different cascading watersheds (a) and a seasonal comparison of carbon source contributions throughout the entire Poyang Lake watershed (i.e., all three cascading watersheds).

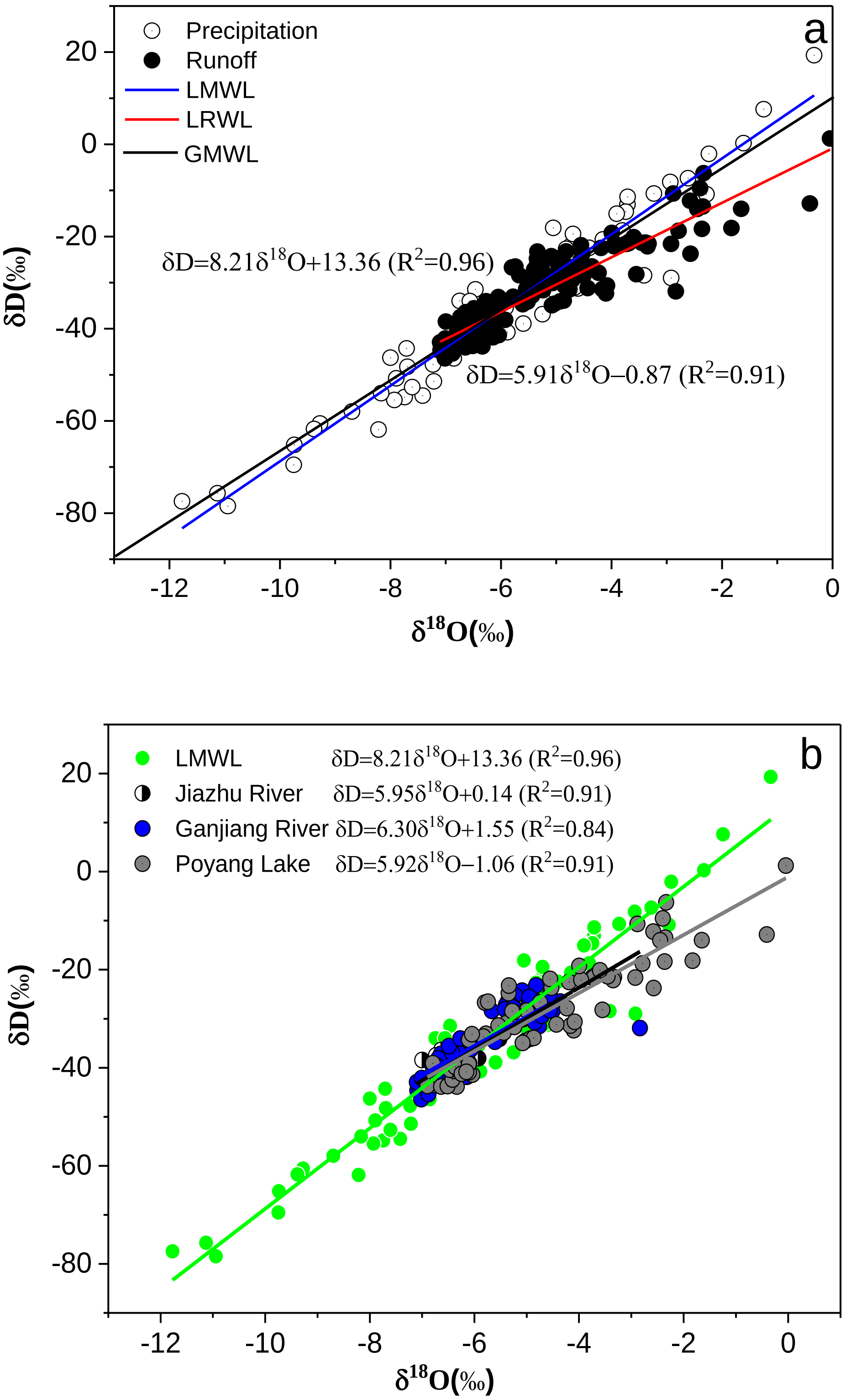

Fig. 6 The Global Meteoric Water Line (GMWL), the Local Meteoric Water Line (LMWL) and the Local Runoff Water Line (LRWL) (a) and the LRWL for the three different watershed sizes (b).

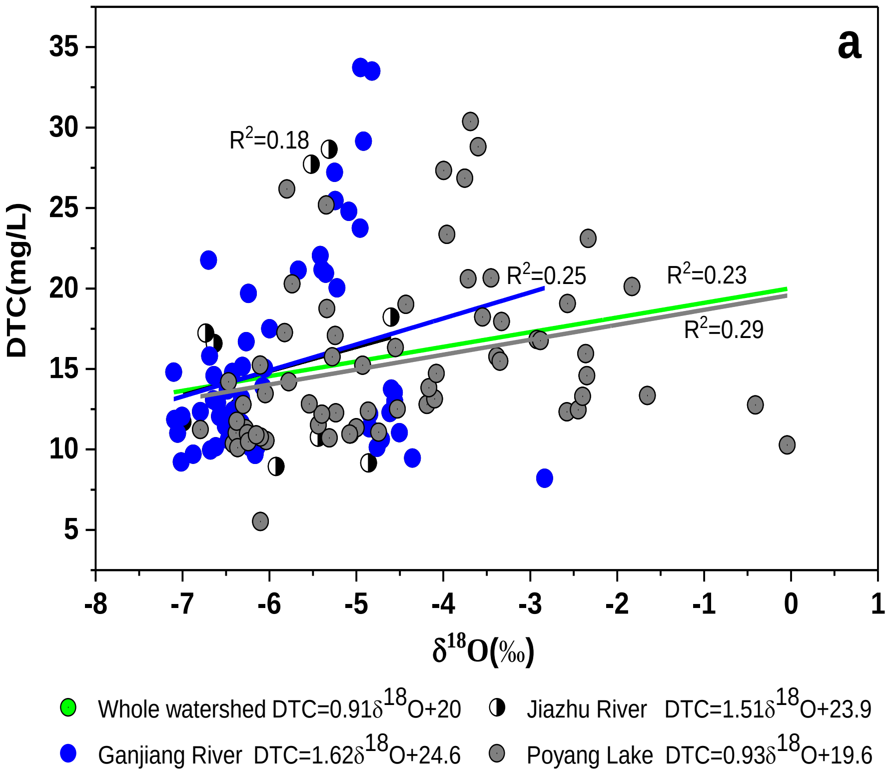
a
DTC(mg/L)
δ18O(‰)
R2=0.18
R2=0.25
R2=0.23
R2=0.29
Whole watershed DTC=0.91δ18O+20
Jiazhu River DTC=1.51δ18O+23.9
Ganjiang River DTC=1.62δ18O+24.6
Poyang Lake DTC=0.93δ18O+19.6

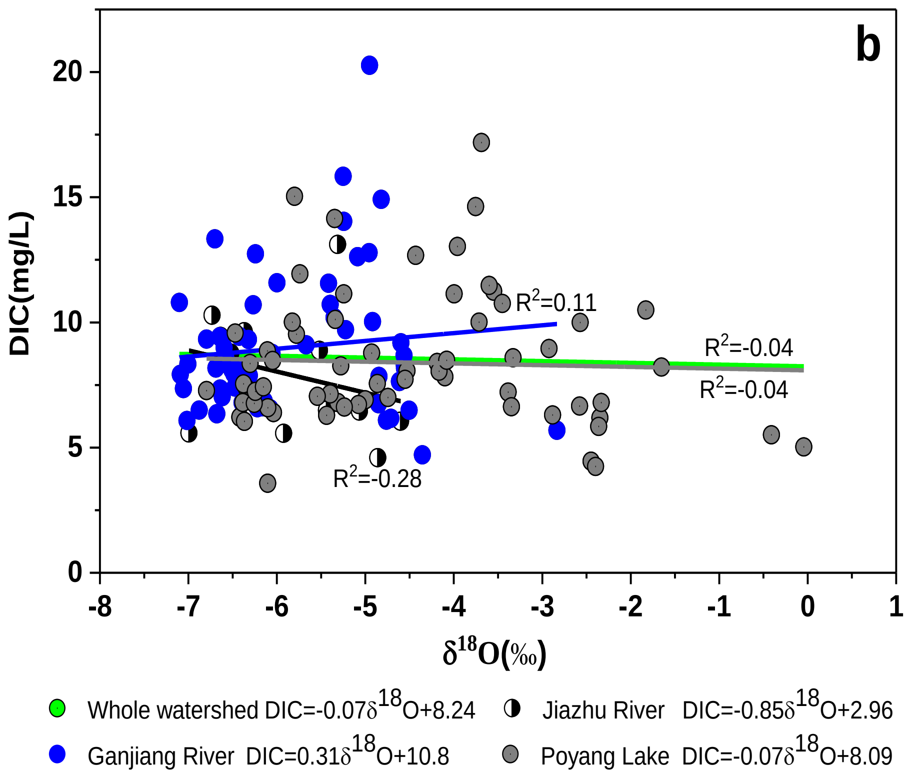
b
DIC(mg/L)
δ18O(‰)
R2=0.11
R2=-0.04
R2=-0.04
R2=-0.28
Whole watershed DIC=-0.07δ18O+8.24
Jiazhu River DIC=-0.85δ18O+2.96
Ganjiang River DIC=0.31δ18O+10.8
Poyang Lake DIC=-0.07δ18O+8.09

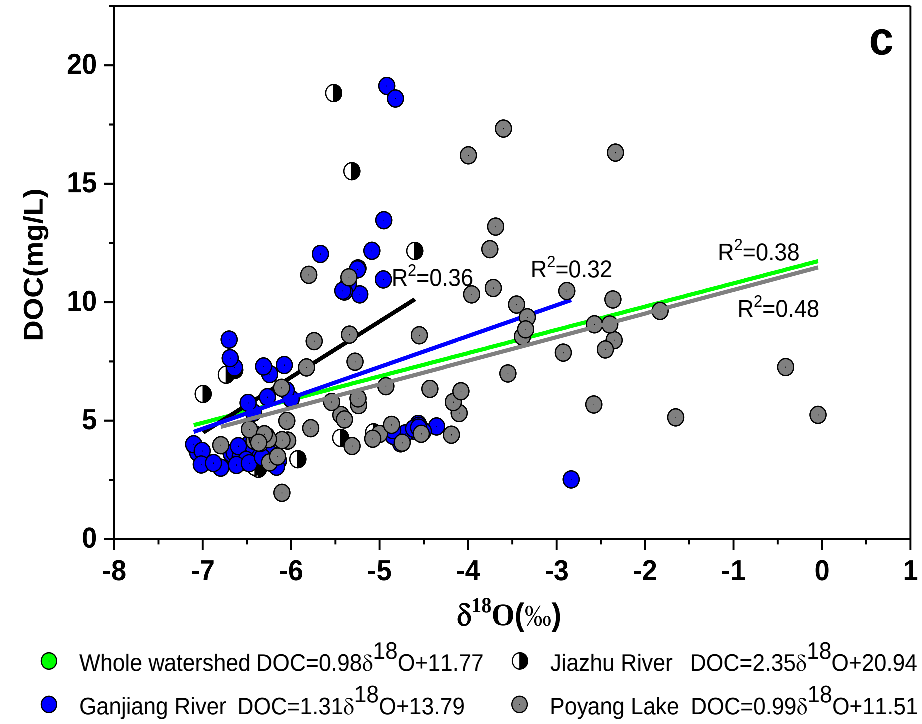

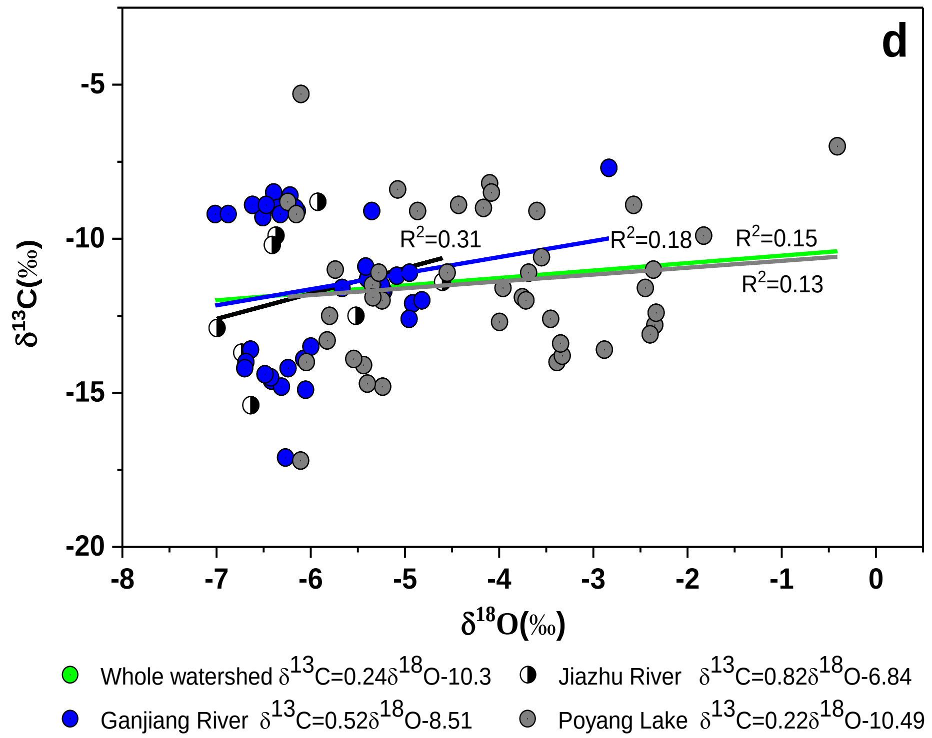

Fig. 7 Correlation analysis values between different carbon sources via runoff at multiple scales and rainfall events: DTC and $\delta^{18}O$ (a), DIC and $\delta^{18}O$ (b), DOC and $\delta^{18}O$ (c) and $\delta^{13}C$ and $\delta^{18}O$ (d).

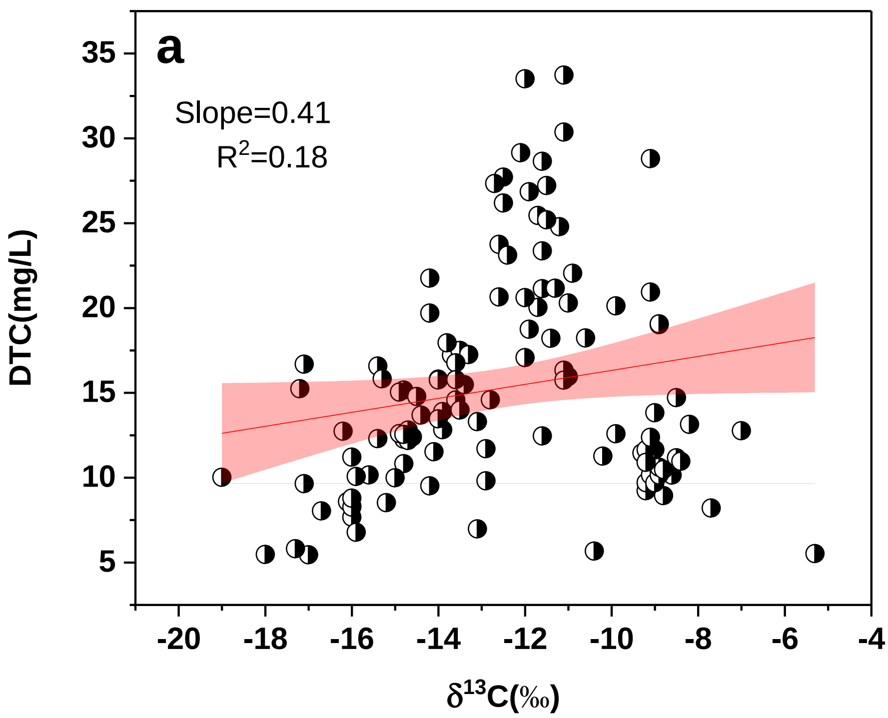
a
Slope=0.41
R2=0.18
DTC(mg/L)
35
30
25
20
15
10
5
-20
-18
-16
-14
-12
-10
-8
-6
-4
δ13C(‰)

615

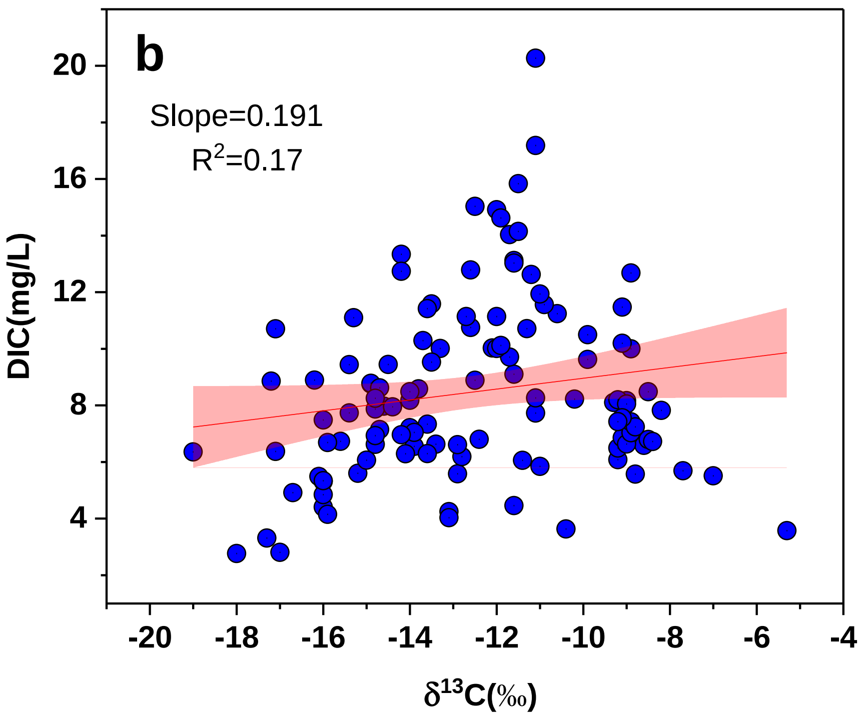
b
Slope=0.191
R2=0.17
DIC(mg/L)
20
16
12
8
4
-20
-18
-16
-14
-12
-10
-8
-6
-4
δ13C(‰)

616

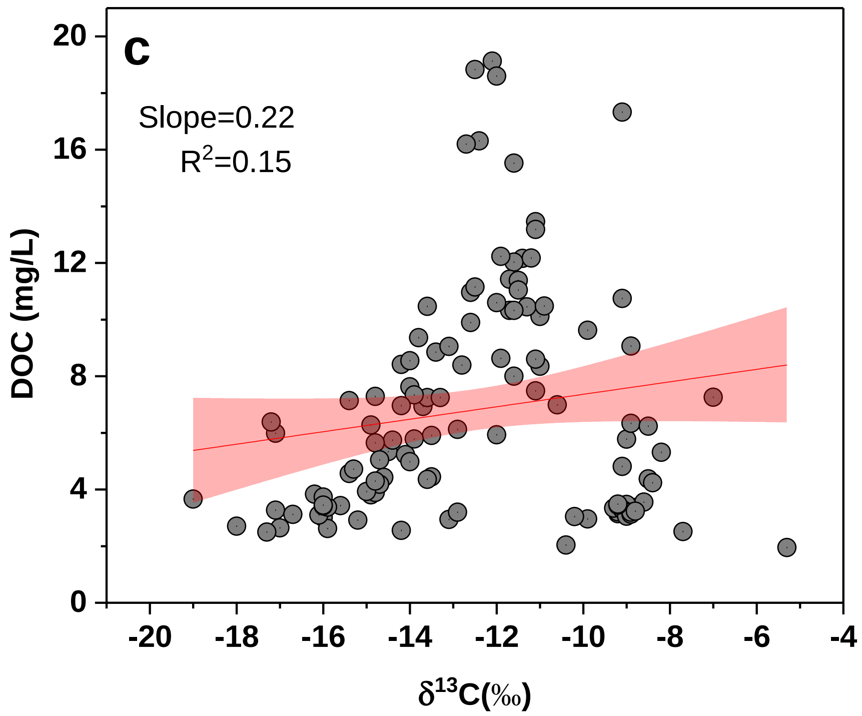

Fig. 8 Correlation analysis values between different carbon forms (DTC (a), DIC (b) and DOC (c)) and $\delta^{13}C$ in runoff.

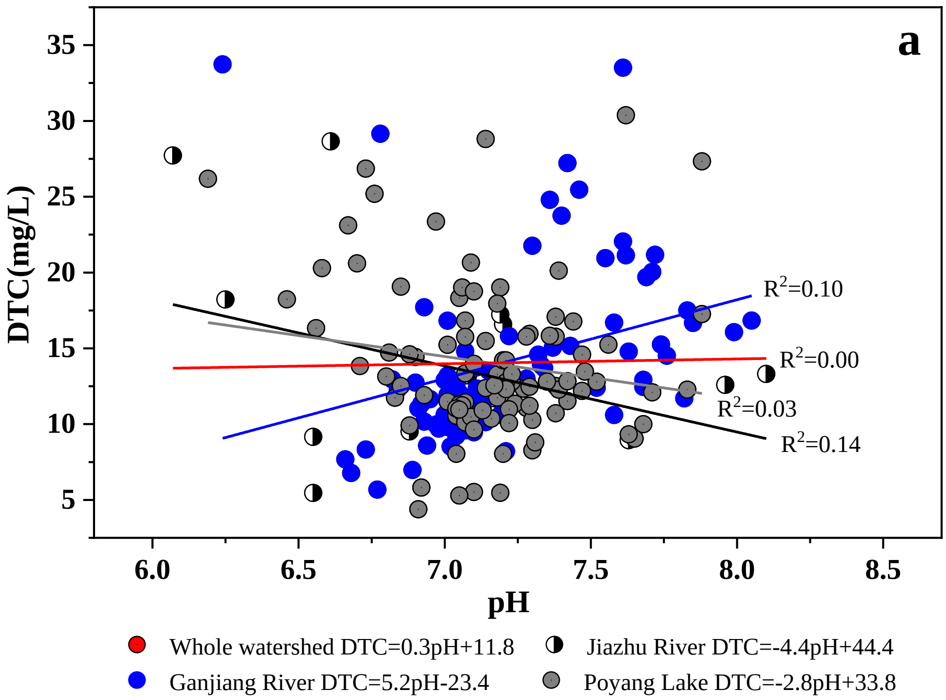
a
DTC(mg/L)
pH
R2=0.10
R2=0.00
R2=0.03
R2=0.14
Whole watershed DTC=0.3pH+11.8
Jiazhu River DTC=-4.4pH+44.4
Ganjiang River DTC=5.2pH-23.4
Poyang Lake DTC=-2.8pH+33.8

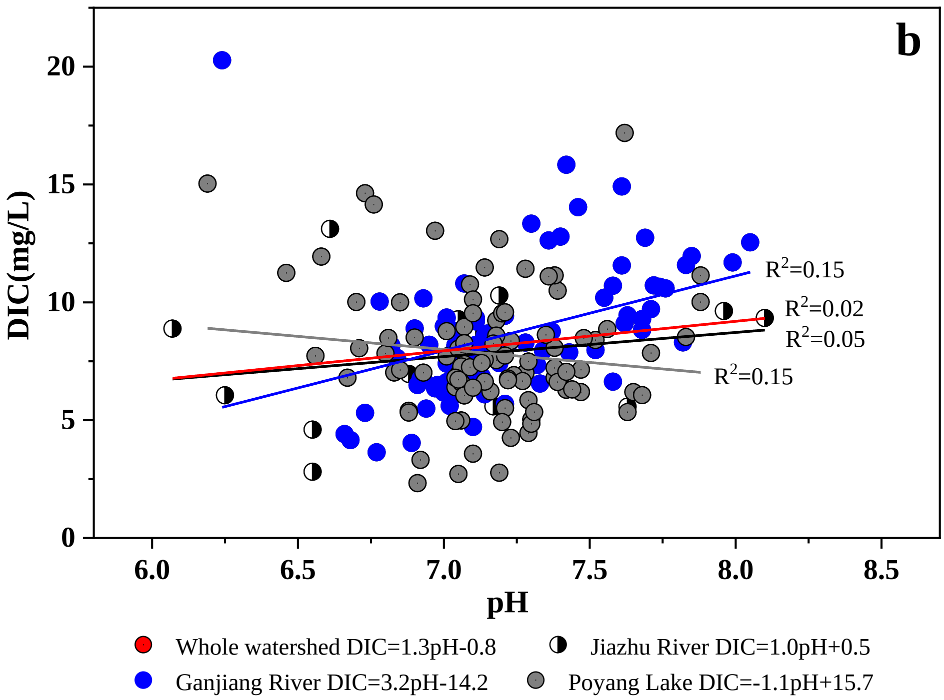
b
DIC(mg/L)
pH
R2=0.15
R2=0.02
R2=0.05
R2=0.15
Whole watershed DIC=1.3pH-0.8
Jiazhu River DIC=1.0pH+0.5
Ganjiang River DIC=3.2pH-14.2
Poyang Lake DIC=-1.1pH+15.7

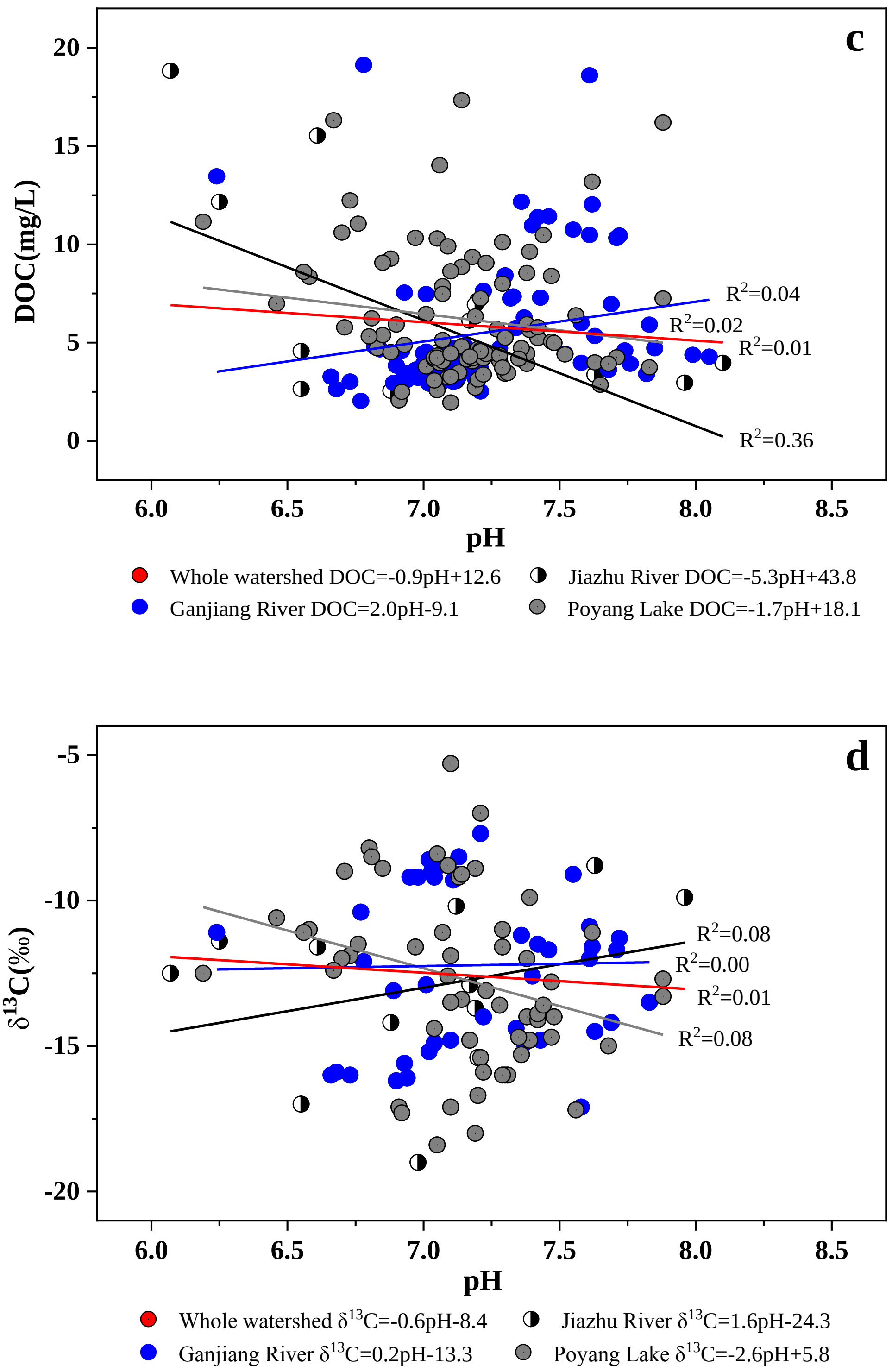

Fig. 9 Correlation analysis of pH and dissolved carbon in rainfall and runoff at multiple scales: DTC and pH (a), DIC and pH (b), DOC and pH (c) and δ^{13}C and pH (d).